α-synuclein—lipoprotein interactions and elevated ApoE level in cerebrospinal fluid from Parkinson's disease patients

Wojciech Paslawski[a,1], Justyna Zareba-Paslawska[a,1], Xiaoqun Zhang[a], Katharina Hölzl[a], Henrik Wadensten[b], Mohammadreza Shariatgorji[b], Shorena Janelidze[c], Oskar Hansson[c,d], Lars Forsgren[e], Per E. Andrén[b], and Per Svenningsson[a,2]

[a]Department of Clinical Neuroscience, Neuro Svenningsson, Karolinska Institute, 171 76 Stockholm, Sweden; [b]Biomolecular Mass Spectrometry Imaging, National Resource for Mass Spectrometry Imaging, Science for Life Laboratory, Department of Pharmaceutical Biosciences, Uppsala University, SE-75124 Uppsala, Sweden; [c]Clinical Memory Research Unit, Faculty of Medicine, Lund University, 221 00 Lund, Sweden; [d]Memory Clinic, Skåne University Hospital, 205 02 Malmö, Sweden; and [e]Department of Pharmacology and Clinical Neuroscience, Umeå University, 901 87 Umeå, Sweden

The progressive accumulation, aggregation, and spread of α-synuclein (αSN) are common hallmarks of Parkinson's disease (PD) pathology. Moreover, numerous proteins interact with αSN species, influencing its toxicity in the brain. In the present study, we extended analyses of αSN-interacting proteins to cerebrospinal fluid (CSF). Using coimmunoprecipation, followed by mass spectrometry, we found that αSN colocalize with apolipoproteins on lipoprotein vesicles. We confirmed these interactions using several methods, including the enrichment of lipoproteins with a recombinant αSN, and the subsequent uptake of prepared vesicles by human dopaminergic neuronal-like cells. Further, we report an increased level of ApoE in CSF from early PD patients compared with matched controls in 3 independent cohorts. Moreover, in contrast to controls, we observed the presence of ApoE-positive neuromelanin-containing dopaminergic neurons in substantia nigra of PD patients. In conclusion, the cooccurrence of αSN on lipoprotein vesicles, and their uptake by dopaminergic neurons along with an increase of ApoE in early PD, proposes a mechanism(s) for αSN spreading in the extracellular milieu of PD.

apolipoproteins | α-synuclein | Parkinson's disease | cerebrospinal fluid

Parkinson's disease (PD) is the second most common neurodegenerative disorder. Its current diagnosis is based on a clinical examination and presence of bradykinesia, rigidity, and resting tremor (1). PD patients also suffer from nonmotor symptoms like depression, hyposmia, sleep disorders, cognitive impairment, and hallucinations (2). PD is confirmed postmortem by a loss of neuromelanin-containing dopaminergic neurons, in the substantia nigra pars compacta (SNc) (3). Several therapies, most of which enhance dopamine neurotransmission, symptomatically relieve motor symptoms of PD, but they do not slow down the progressive neurodegeneration (4). A second pathological hallmark of PD is the presence of abnormal α-synuclein (αSN)-enriched inclusions called Lewy bodies (5).

Physiological αSN has been proposed to engage in synaptic vesicle trafficking, exocytosis, regulation of neurite outgrowth, and nerve cell adhesion (6–8). αSN monomers are unstructured under physiological conditions (9), but can associate into oligomeric (10, 11) and amyloid species (5). It has been shown that αSN aggregates are able to disrupt cell membranes (12) and spread from cell to cell (13). αSN not only self-assemble into aggregates but also interact with a number of proteins within nerve cells, including parkin, β-amyloid, dopamine transporter, tau, 14-3-3, caveolin-1, and tubulin (14–17). The corresponding knowledge about αSN interactions with extracellular components remains sparse.

Cerebrospinal fluid (CSF) reflects important aspects of the extracellular milieu of the brain. Moreover, CSF studies have provided several clinically meaningful biomarkers for the diagnosis and prognosis of neurological disorders, including Alzheimer's disease,

multiple system atrophy (MSA), and progressive supranuclear palsy (PSP) (18, 19). Alterations in the levels of αSN species in CSF from PD patients have been reported, but the magnitude and/or reproducibility of reported changes varies considerably (20, 21). In the present study, our aim was to identify αSN-interacting proteins in CSF and quantify their levels in CSF from PD patients along with age- and gender-matched controls. Moreover, we examined content validity of identified αSN interactors by studying a dopaminergic cell line and human brain tissue from SNc.

Materials and Methods

Subjects and Sample Collections. Subjects' consent was obtained according to the Declaration of Helsinki. All experiments involving human subjects were approved by the regional ethical committees at Karolinska University Hospital, Umeå University, and Lund University (2016/19-31/1, 2014-163-31M, 2012/2224-32/4, 2011-334-31M, 09-160M, and 2008-290). Samples were collected as described before (22–24). Briefly, the standardized lumbar puncture procedure was performed sitting up, in accordance with the Alzheimer's Disease Neuroimaging Initiative recommended protocol. The first 2 mL of sample

---

Significance

Two of the most important issues in Parkinson's disease (PD) research are the identification of mechanisms underlying α-synuclein cell-to-cell transfer in the nervous system and the discovery of early diagnostic biomarkers. Both of these issues are addressed in our current manuscript. Using multiple approaches, we present that α-synuclein interacts with lipoproteins within human cerebrospinal fluid and can be taken up by cells in such a state. Moreover, using cerebrospinal fluid samples from 3 large and independent cohorts of patients, we demonstrate that apolipoprotein E is elevated in early, not yet medicated, patients with PD. Finally, using postmortem brain tissue, we provide preliminary histological evidence that apolipoprotein E is enriched in a subpopulation of dopaminergic neurons of human substantia nigra.

---

were discarded, and between 10 and 12 mL of CSF was collected. Cell counts were measured, samples were centrifuged, aliquoted, frozen on dry ice, and stored. Time between sample collection and freezing was maximum 30 min. Blood-contaminated samples were excluded. Formalin-fixed, paraffin-embedded 5-μm human brain sections, from subjects without neurological disorders (n = 2; male, age 77 y and male, age 73 y) or PD (n = 2; male, age 78 y, disease duration 12 y and male, age 75 y, disease duration 12 y), were obtained from the Brain Bank at Karolinska Institutet.

Chemicals and Antibodies. Unless stated otherwise, all chemicals were purchased from Sigma-Aldrich (Merck KGaA) and were of an analytical grade. All solutions were prepared using Milli-Q deionized water (Millipore). The recombinant ApoE was purchased from Sigma-Aldrich (SRP4696, Merck KGaA). The list of antibodies, and methods in which they were used, can be found in *SI Appendix*, Table S1.

Coimmunoprecipitation. Protein A/G agarose beads (Abcam) were pretreated with 1% BSA, dissolved in phosphate-buffered saline (PBS) buffer (20 mM phosphate, 150 mM NaCl, pH-7.4), to block any unspecific interactions. A large volume of CSF (50 mL) was pulled down from healthy controls, and endogenous immunoglobulins were depleted from the sample during 2-h incubation with protein A/G agarose beads, followed by elimination of beads via centrifugation. The antibody recognizing αSN, used for similar approaches previously (25–27), was added to the obtained solution and incubated overnight in 4 °C. Thereafter, the sample was incubated for 6 h with protein A/G agarose beads at room temperature (RT) and spun. The beads were washed, and protein elution was conducted by 0.2 M glycine pH 2.6. The sample was dialyzed, lyophilized, and stored at −20 °C for further analysis. In parallel, separate positive and negative control samples were prepared. Recombinant αSN served as a positive control. The negative control was a CSF sample without addition of the primary anti-αSN antibody.

ApoE Depletion. Depletion of ApoE-positive vesicles from human CSF was performed using the aforementioned coimmunoprecipitation (co-IP) approach; 200 μL of CSF was used as a starting material. The procedure was terminated after collecting the supernatant obtained after removal of protein A/G agarose beads bound to the anti-ApoE antibody.

ELISA. A microtiter plate was coated with the capture antibody at 10 μg/mL concentration in carbonate/bicarbonate buffer (pH 9.6) and incubated overnight at 4 °C. Next, the plate was washed with PBS containing 0.1% (vol/vol) Tween-20 (PBS-T), and remaining protein-binding sites were blocked for 2 h at RT with 5% nonfat dry milk in PBS. The plate was washed with PBS-T, and 10 μL of each sample diluted in PBS, with or without addition of the detergent, was incubated for 2 h at 37 °C and washed with PBS-T. Subsequently, a detection antibody was added to each well, incubated for 2 h at RT, and washed with PBS-T. A secondary antibody was added to each well, incubated for 1 h at RT and washed with PBS-T. Then 3,3′,5,5′-Tetramethylbenzidine solution (10 μg/mL in 0.05 M phosphate-citrate buffer, pH 5.0) was added to each well and incubated for 30 min. Equal volume of a

stopping solution (2 M H_2SO_4) was added to each well and the optical density was read at 450 nm. For detection of αSN before and after depletion of ApoE-positive vesicles chemiluminescent substrate (Thermo Fisher Scientific SuperSignal ELISA Pico Substrate, Thermo Fisher Scientific) was used instead of 3,3′,5,5′-Tetramethylbenzidine solution.

Mass Spectrometry. IP samples were digested using modified trypsin (Promega). Obtained peptides were purified using C18 resin ZipTips (Millipore). All samples were dried down to approximately 10 μL using a vacuum centrifuge. Thereafter, samples were analyzed on a nanoLC system (Easy-nLC II; Thermo Fisher Scientific) coupled to an electrospray linear ion trap (LTQ; Thermo Fisher Scientific) mass spectrometer. The acquired mass spectrometry (MS)/MS data were converted into a combined mgf-file. The mgf-files were searched against *Homo sapiens* Database using a X!Tandem search engine.

Immunogold Labeling and Transmission Electron Microscopy. To remove excess proteins and analyze mostly vesicles, the CSF sample was initially filtered, and the retained solution was collected for transmission electron microscopy (TEM) analysis. An aliquot from each sample was added to a grid, and the excess solution was soaked off by a filter paper. The samples were incubated with primary antibodies for 1.5 h, grids were rinsed, and the secondary antibodies were added: goat polyclonal anti-mouse (5 nm, anti-ApoE antibody detection) or goat polyclonal anti-rabbit (10 nm, anti-αSN antibody detection) antibodies at a final dilution of 1:100 each. The samples were examined at 80 kV.

SDS/PAGE. SDS/PAGE was performed as described before (28). Briefly, the sample was mixed with a denaturing loading buffer and boiled at 95 °C for 5 min. For analysis of samples containing αSN oligomers or fibrils, the denaturing loading buffer was additionally supplemented with urea to 10 M final concentration, and incubation in 95 °C for 5 min was changed to 65 °C for 60 min to allow dissociation of aggregates. Next, samples were separated using a bis-Tris acrylamide gel using 2-(N-morpholino)ethanesulfonic acid running buffer. If necessary, the gel was stained using Coomassie Brilliant Blue (CBB) R-250 solution.

Western Blotting. After SDS/PAGE, gels were assembled with 0.45-μm pore size polyvinylidene difluoride membranes and overnight transfer was performed at 4 °C. Membranes were blocked during 1-h incubation in 5% skim milk at RT. Next, membranes were incubated overnight at 4 °C with a primary antibody diluted 1:2,000 (vol/vol) in 1% skim milk. Membranes were thereafter incubated for 2 h with appropriate horseradish peroxidase (HRP)-conjugated secondary antibody (Dako) diluted 1:10,000 (vol/vol) in 1% skim milk at RT. The signal was developed by a Clarity Western ECL Substrate (Bio-Rad), specificity of antibodies was checked (*SI Appendix*, Fig. S1), and levels of visualized proteins were estimated by measuring band intensities with ImageJ (29). A colorimetric scan was used to visualize the protein ladder.

Immunohistochemistry. Human formalin-fixed, paraffin-embedded 5-μm sections were deparaffinized and rehydrated, and epitope retrieval was performed on each section. The endogenous peroxidase activity was quenched, and

Table 1. Proteins identified using MS after IP against αSN from the human CSF

Sample	log(e)	log(I)	PCM	PCC	UP	MW	Description
CSF IP	−188.3	7.05	52	67	14	36.1	APOE:p, apolipoprotein E
	−141	5.62	71	82	11	11.4	SNCA:p, synuclein alpha
	−132.1	5.28	18	21	10	69.2	Serum albumin, bovine; BSA
	−104.2	6.84	35	44	9	30.8	APOA1:p, apolipoprotein A1
	−43.9	7	12	29	4	52.5	ApoJ:p, apolipoprotein J
	−20.2	4.8	12	15	2	24.4	Trypsin; EC 3.4.21.4
	−14.8	4	24	33	2	12.6	IGHV@:p, Ig heavy variable 3-23
Negative control IP	−52	4.47	8.8	16	5	41.3	Ig heavy constant gamma 3
	−4.7	4.11	4.7	7	1	24.5	Bovine Alpha-S1-casein
	−4.6	3.28	2.6	4	1	36.6	IGHA2:p, Ig heavy constant α 2
Positive control Recombinant αSN IP	−145	5.15	71	82	11	11.4	SNCA:p, synuclein alpha
	−15.1	3.76	24	33	2	12.6	IGHV@:p, Ig heavy variable 3-23

Proteins identified in CSF samples, a specificity control, i.e., the sample without the αSN antibody and a positive control, i.e., samples spiked with recombinant αSN; log(e), base-10 log of the expectation that this assignment is stochastic; log(I), base-10 log of the sum of the intensities of the fragment ion spectra; PCM, protein coverage measured; PCC, protein coverage corrected; UP, number of unique peptides found; MW, molecular weight (kilodaltons).
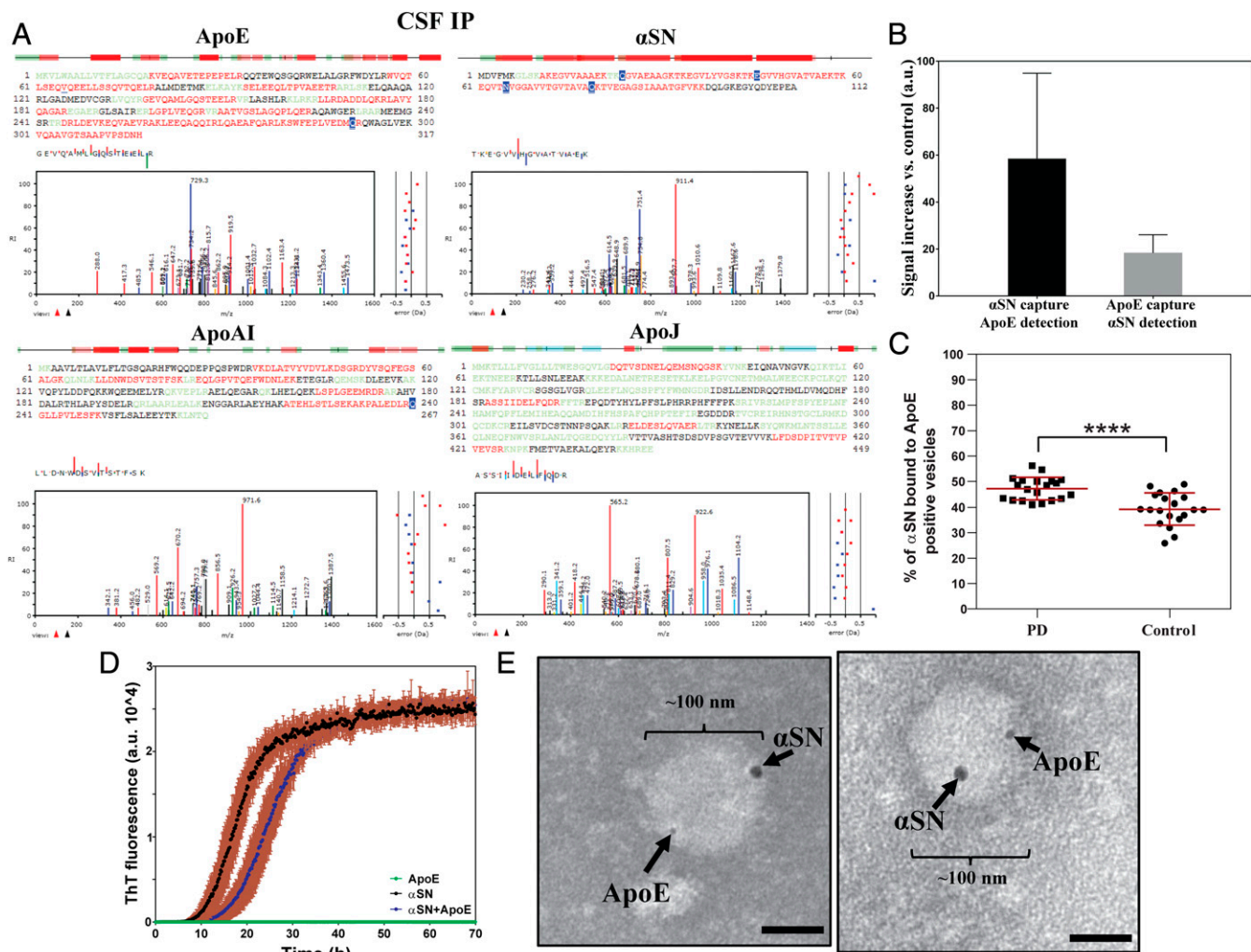
Fig. 1. Analysis of the ApoE colocalization with αSN on vesicles from the human CSF. (*A*) αSN and identified apolipoproteins sequences' coverages, and selected peptides spectra obtained after trypsin cleaved peptides' fragmentation for each protein, for CSF samples after IP against αSN. Red, residues from a peptide domain observed at least once during the analysis; green, residues predicted to be difficult to observe by standard techniques; blue, residues found are chemically modified. (*B*) A codetection of ApoE and αSN using ELISA. Black bar, the detection of ApoE on anti-αSN antibody-bound complexes; gray bar, the detection of αSN on anti-ApoE antibody-bound complexes. (*C*) Levels of αSN bound to ApoE-positive vesicles in CSF from healthy controls compared with PD patients from the Stockholm cohort. Analysis was performed using the Mann–Whitney *U* test. *P* value < 0.05 was considered statistically significant. ****$P < 0.0001$. (*D*) The aggregation profile of the aggregation of ApoE alone (green), the aggregation of αSN alone (black), and the aggregation of αSN mixed with ApoE (blue). Each point represents the mean of 4 replicates, and errors bars represent SD of measurements. Comparison of the signal at plateau and the lag phase of aggregation between αSN with and without addition of the recombinant ApoE was performed using the Mann–Whitney *U* test. *P* value < 0.05 was considered statistically significant. (*E*) TEM images with the immunogold labeling representing αSN and ApoE colocalization on extracellular vesicles in the human CSF. (Scale bars, 50 nm.)

unspecific interactions were blocked using 5% goat normal serum followed by overnight incubation with the anti-ApoE antibody. Thereafter, sections were incubated with the HRP-conjugated secondary antibody, and the peroxidase labeling was visualized with a mix of 3,3-diaminobenzidine and nickel (SK-4100; Vector Laboratories), which yielded a blue/gray reaction product.

Densitometry. The optical density of ApoE immunoreactivity was performed on representative light microscopy pictures. The digital images of SN were obtained by a high-power objective lens (40×, CFI Plan Apo Lambda; Nikon) and analyzed by ImageJ in grayscale. From each picture, 6 random neuromelanin-positive cells were selected. The intracellular signal was measured within the cell body in the region where no neuromelanin was present. The extracellular signal was measured in the parenchyma just next to the cell of interest. The optical density for each cell was corrected for nonspecific background density. The data are presented as arbitrary units or intracellular/extracellular signal ratio.

Preparation of the Recombinant αSN Monomers, Oligomers, and Fibrils. The recombinant human αSN was expressed in *Escherichia coli* and purified as described before (11). Briefly, cells were harvested and lysed. The majority of

unwanted proteins were precipitated by acidification. The solution was fractionated on a Q-Sepharose column. Fractions containing αSN were identified by SDS/PAGE and pulled together, and high molecular weight aggregates were removed by filtration. αSN oligomers were prepared by dissolving αSN monomers at 12 mg/mL followed by incubation at 37 °C with shaking. Insoluble material was removed, and supernatant was fractioned using Superpose 6 column (GE Healthcare). Oligomer fractions were collected, concentrated, and stored at 4 °C. The recombinant αSN was fibrillated by dissolving αSN monomers at 1 mg/mL and incubated at 37 °C with shaking for 5 d. Obtained samples were centrifuged, obtained pellet was suspended in PBS buffer, and preformed fibrils (PFF) were prepared by sonicating the sample to obtain unified length of fibrils. For aggregation analysis, samples were incubated with or without addition of ApoE, at a final concentration of 1 mg/mL for αSN and 0.25 mg/mL for ApoE with 40 μM ThT in a Tecan Spark 10 M (Tecan Nordic AB) plate reader at 37 °C with shaking. The ThT signal was monitored at 448-nm excitation and 485-nm emission.

Preparation of Enriched Lipoprotein Vesicles. Human plasma high-density lipoprotein (HDL) (437647) and very low-density lipoprotein (VLDL) (437641)

vesicles were purchased from Merck Millipore. For the enrichment, 550 µg/mL (cholesterol content) lipoproteins were mixed with αSN or ApoE (11 µM final concentration each) and incubated for 1 h at 37 °C. For the enrichment with both αSN and ApoE, αSN was added first and incubated for 1 h at 37 °C, followed by 1-h incubation with ApoE. Unbound proteins were removed by passing the solution through 100-kDa or 50-kDa Amicon Ultra-0.5 Centrifugal Filter Units (Millipore). Finally, the sample was washed 3 times by adding PBS to the retained fraction and passing the solution through 100-kDa or 50-kDa Centrifugal Filter Units.

Lipoprotein Uptake by Dopaminergic Cells. SH-SY5Y human neuroblastoma cells were routinely maintained in a Dulbecco's Modified Eagle Medium (DMEM) modified medium supplemented with fetal bovine serum (FBS) (10%), L-alanyl-L-glutamine (2 mM), penicillin (100 µg/mL), and streptomycin (100 µg/mL). Cultures were maintained at 37 °C in 5% CO_2/humidified air. For the uptake screening, cells were cultured in 24-well plates on laminin-coated cover glasses at a seeding density of 1×10^5 cells per well in a differentiating medium (DMEM modified medium supplemented with FBS [1%], L-alanyl-L-glutamine [2 mM], penicillin [100 µg/mL], streptomycin [100 µg/mL], and 10 µM retinoic acid) for 4 d. Human plasma HDL (437647; Merck Millipore), VLDL (437641; Merck Millipore), and the recombinant αSN were marked with Alexa Fluor 568 NHS-ester (A20003; Thermo Fisher Scientific) or Alexa Fluor 488 NHS-ester (A20000; Thermo Fisher Scientific) according to the manufacturer protocol. For uptake study, cell medium was changed to DMEM modified medium supplemented with FBS (0.1%), L-alanyl-L-glutamine (2 mM), penicillin (100 µg/mL), streptomycin (100 µg/mL), and 10 µM retinoic acid. Labeled human plasma HDL and VLDL, with or without enrichment with the labeled monomeric αSN (enrichment protocol described above), the labeled monomeric αSN, and vehicle controls were added to cells (final concentrations: 20 µM cholesterol and 1 µM αSN) and incubated for 4 h. Next, cells were washed with PBS and fixed with 4% paraformaldehyde. Subsequently, cells were stained with the Alexa Fluor 647 phalloidin dye (A22287; Thermo Fisher Scientific) according to the manufacturer protocol followed by a DAPI counterstaining. The single-plane images of cells were obtained using a confocal microscopy (LSM880; Zeiss).

Separation of Lipoproteins by Density-Gradient Ultracentrifugation. Lipoproteins were isolated from 0.1 mL of αSN–lipoprotein mix by KBr-density gradient ultracentrifugation according to Redgrave et al. (30). Briefly, after incubation, density and volume of each sample was adjusted, respectively, to 1.21 g/mL and 1 mL with KBr and transferred into centrifuge tubes. A discontinuous density gradient was formed by layering 3 mL of 1.063 g/mL salt solution above the sample, followed by 3 mL of 1.019 g/mL salt solution and 3 mL of 1.006 g/mL salt solution. Salt solutions were prepared from KBr and NaCl and contained 0.1 mg/mL 2,2′,2′′,2′′′-(ethane-1,2-diyldinitrilo)tetraacetic acid. The samples were centrifuged at 386,000 × g for 24 h at 20 °C. The 1.25-mL fractions were collected and analyzed using the Western blotting (WB) method.

Size-Exclusion Chromatography. The αSN–lipoprotein samples were analyzed and fractionated using Superose 6 Increase 10/300 GL column connected to an ÄKTA Explorer system (GE Healthcare) using PBS as a mobile phase. The appearance of proteins was monitored by reading the absorbance at 280 nm. Obtained fractions were collected and analyzed using the WB method.

Sample Randomization. For each patient cohort, all available samples were chosen taking age and gender matching into consideration. Obtained CSF and plasma samples were coded and analyzed blindly. No sample was excluded from the final analysis. Samples were decoded after experimental data were obtained.

Statistics. Statistical analyses were performed using a GraphPad Prism software (GraphPadInc). Comparison between 2 groups was performed using a Mann–Whitney U test. Multiple comparison was performed using a Kruskal–Wallis H test with a Dunn's correction. A Spearman's rank correlation coefficient was used to analyze dependence between 2 sets of data. All statistical tests were 2-tailed, and P value < 0.05 was considered statistically significant.

Data Availability. The data are available upon reasonable request. Due to sensitive nature of the patients' clinical information, the ethics protocol does not allow open data sharing.

For more detailed description of the methods, see *SI Appendix*.

Results

αSN Colocalizes with Apolipoproteins in the Human CSF.
Data on αSN interactors in the extracellular milieu including CSF are sparse. Therefore, we performed co-IP (*SI Appendix*, Fig. S2) against αSN on CSF samples, and analyzed bounded proteins using MS. Unexpectedly, our data showed that αSN-bound proteins in CSF were mainly apolipoproteins, among which ApoE was the most apparent. Moreover, we identified ApoAI- and ApoJ-derived peptides (Table 1, Fig. 1A, and *SI Appendix*, Fig. S3). Neither αSN- nor apolipoproteins-related peptides were identified in the negative control (Table 1).

To confirm the co-IP of αSN and ApoE, we performed ELISA on crude CSF samples using 2 reciprocal settings: First, a capture was made with an anti-αSN antibody and detection was performed with an anti-ApoE antibody; second, proteins were captured using the antibody against ApoE, and detection was performed using the antibody against αSN. With both settings, we observed a clear ELISA signal (Fig. 1B), indicating that ApoE and αSN closely interact in CSF. Moreover, we did not observe any unspecific interactions when using antibody controls (rabbit and goat IgGs), in the ELISA approach, neither for recombinant proteins nor for CSF samples (*SI Appendix*, Fig. S4). Furthermore, analysis of our data suggests that around 40 to 50% of CSF αSN is associated with ApoE-positive lipoproteins (*SI Appendix*, Fig. S4D).

To confirm this finding, we performed analysis of αSN levels before and after depletion of ApoE-positive vesicles in CSF from 20 healthy controls (14/6 males/females, average age 64.10 ± 8.42 y) and 20 PD patients (14/6 males/females, average age
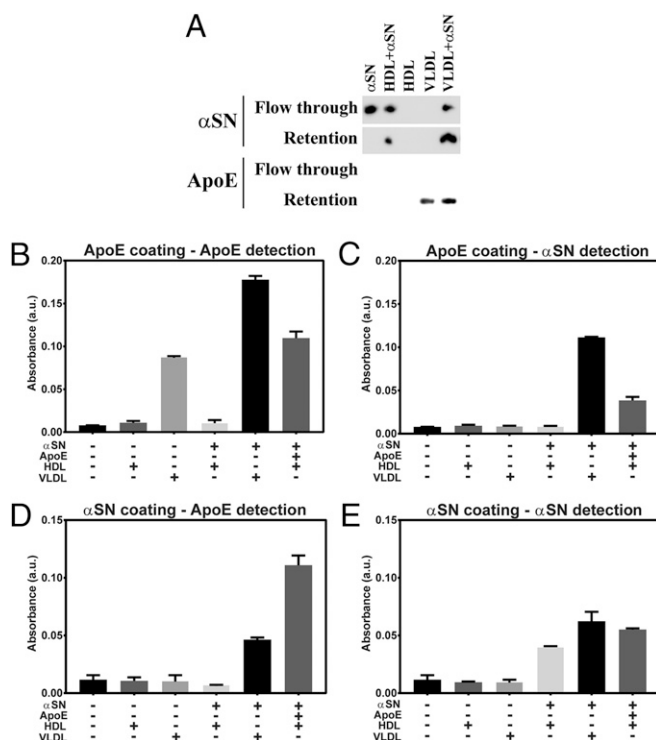

Fig. 2. Enrichment of lipoprotein vesicles with αSN. (A) The WB analysis against αSN and ApoE of flow-through and retained fractions obtained after lipoprotein enrichment with αSN and subsequent filtration through 100-kDa spin filter. (B–E) The ELISA analysis of fractions retained on the filter after enrichment of HDL and VLDL vesicles with αSN and/or ApoE. Corresponding graphs represent ELISA analyses using (B) the anti-ApoE capture and the anti-ApoE detection antibody, (C) the anti-ApoE capture and the anti-αSN detection antibody, (D) the anti-αSN capture and the anti-ApoE detection antibody, and (E) the anti-αSN capture and the anti-αSN detection antibody.

62.65 ± 12.72 y). We observed a decrease of αSN in samples from both PD and control subjects (Fig. 1C and *SI Appendix*, Fig. S5). Moreover, the amount of αSN bound to ApoE-positive vesicles was significantly higher in PD cases compared with healthy controls (Fig. 1C).

To investigate whether the interaction between αSN and ApoE is direct or indirect, we analyzed kinetics of αSN fibril formation after addition of recombinant ApoE. We did not observe any significant changes in the aggregation profile of the recombinant αSN, suggesting indirect contact between these proteins (Fig. 1D).

To further examine the character of interactions observed between αSN and ApoE, we performed TEM analysis on CSF samples. Indeed, αSN and ApoE double immune-gold labeling revealed a colocalization of αSN and ApoE on larger (>30 nm) vesicular structures in CSF (Fig. 1E and *SI Appendix*, Fig. S6A). However, it is possible that the αSN and ApoE colocalization also occurred on smaller vesicles, but, due to a steric hindrance, caused by a relatively large size of immunogold particles and antibodies, only a single protein could be detected on vesicles smaller than 30 nm in size (*SI Appendix*, Fig. S6B).

No clear lipid bilayer was observed on αSN- and ApoE-positive vesicular structures in TEM analysis (Fig. 1E), suggesting that they are lipoprotein vesicles. This is in accordance with the data from the MS analysis identifying only lipoproteins' markers (Table 1, Fig. 1A, and *SI Appendix*, Fig. S3). We therefore investigated the ability of αSN to interact with lipoprotein vesicles in vitro. Considering that CSF lipoproteins are predominantly of the size and density of plasma HDL, human plasma HDLs were included in the study. Moreover, due to fact that CSF HDLs are mainly ApoE-positive, contrary to plasma HDL which are mainly ApoAI-positive (31), human plasma VLDL were also used to address the role of ApoE-positive lipoproteins. Accordingly, we incubated human plasma HDL or VLDL vesicles with recombinant monomeric αSN and passed the obtained samples through a size-exclusion filter. Subsequent WB analysis of eluates showed that the recombinant monomeric αSN without vesicles passed entirely through the filter, while a large amount of αSN incubated with either HDL or VLDL vesicles was retained on the filter. This confirmed αSN binding ability to lipoprotein vesicles (Fig. 2A).

To verify that αSN and ApoE might colocalize on the lipoproteins resembling CSF lipoproteins, we performed double enrichment of plasma HDL and examined whether αSN- and/or ApoE-enriched vesicle can be detected by ELISA settings applied in the CSF study. When using both capture and detection antibodies against ApoE, we obtained signal for VLDL, VLDL+αSN, and HDL+αSN+ApoE vesicles (Fig. 2B). For the anti-ApoE capture antibody and the anti-αSN detection antibody,

the signal was observed for VLDL+αSN and HDL+αSN+ApoE vesicles (Fig. 2C). For the anti-αSN capture antibody and the anti-ApoE detection antibody, the ApoE signal was observed for VLDL+αSN and HDL+αSN+ApoE vesicles (Fig. 2D). When using both capture and detection antibodies against αSN, we obtained signal for VLDL+αSN, HDL+αSN, and HDL+αSN+ApoE vesicles (Fig. 2E). We extended our examination of αSN and lipoproteins interactions to include not only monomeric αSN but also oligomeric and PFF αSN, using 2 additional methods. First, instead of filtration technique, we performed density gradient ultracentrifugation separation followed by WB analysis (*SI Appendix*, Fig. S7). In this experiment, we were able to detect the 3 forms of αSN both in protein and lipoprotein fractions. We conclude that not only monomeric but also oligomeric and PFF forms of αSN can interact with lipoproteins. The fact that ultracentrifugation detached apolipoproteins from vesicles is in agreement with previous reports (32) (*SI Appendix*, Fig. S7). Therefore, to omit detachment of proteins from vesicles, we decided to use a size-exclusion chromatography (SEC) approach, which does not introduce any excessive forces to the sample separation. As described above, human plasma HDL or VLDL vesicles were incubated with each of the 3 forms of αSN separately and injected to the column for SEC analysis. We observed a shift in retention volume after αSN and lipoprotein coincubation, indicating formation of larger-size complexes (*SI Appendix*, Fig. S8). We further confirmed that both αSN and lipoproteins are present in fractions collected from shifted peaks, using the WB method, verifying interactions of monomeric, oligomeric, and PFFs forms of αSN with lipoproteins.

Moreover, using a filtration method with spin filters, presented in Fig. 2, and SEC, we confirm that such isolation of lipoproteins enriched with monomeric αSN does not affect the interaction between monomeric αSN and lipoproteins (*SI Appendix*, Fig. S9).

Based on the obtained results, we decided to investigate whether ApoE, and other identified apolipoproteins, are changed in the CSF and plasma from PD patients and examine their biomarker potential.

Increased Level of ApoE in CSF, but Not in Plasma, from PD Patients. ApoE is the main apolipoprotein in central nervous system (CNS), and its allelic variants are strongly implicated in the pathogenesis of Alzheimer's disease (33, 34). There is also some evidence that allelic variants of ApoE predispose to dementia in PD (35). However, no study has reported changes in ApoE protein level in CSF or plasma from PD patients. Therefore, we measured ApoE in biofluids from PD patients and from matched controls (*SI Appendix*, Tables S2 and S3). Throughout the ELISA optimization process, we realized that the level of ApoE detected by ELISA in the human CSF rises with increasing concentration

Table 2. Results from the statistical analysis of differences in apolipoproteins levels in CSF and plasma samples, between PD patients and matched controls from the Stockholm cohort

| | Mann–Whitney | | Kruskal–Wallis | | | | | |
| | | | CSF | | | Plasma | | |
Analyzed apolipoprotein	CSF Control vs. PD	Plasma Control vs. PD	Control vs. PD treated	PD treated vs. PD untreated	Control vs. PD untreated	Control vs. PD treated	PD treated vs. PD untreated	Control vs. PD untreated
ApoAI	0.7995	**0.0048**	>0.9999	>0.9999	>0.9999	0.0598	>0.9999	0.0697
ApoCI	0.4245	0.6176	0.0807	**0.0439**	>0.9999	>0.9999	0.1918	0.5398
ApoE	**<0.0001**	0.8194	**0.0023**	0.2830	**<0.0001**	0.7492	0.4278	>0.9999
ApoJ	**0.0116**	0.639	**0.0413**	>0.9999	0.2601	>0.9999	0.4312	0.7826

The left part of the table represents *P* values obtained after analyzing apolipoproteins' levels in PD (PD) patient set vs. healthy controls (the Mann–Whitney *U* test). The right part of the table represents *P* values obtained after splitting the PD group into treated and untreated patients' subsets and analyzing apolipoproteins' levels between them and vs. healthy controls (the Kruskal–Wallis H test with a Dunn's correction). *P* values < 0.05 are considered significant and are marked with a bold font.

of detergents in a buffer, up to the point where the detergent concentration is too high for the method to work at all. At the same time, the level of recombinant ApoE, detected with ELISA method, was independent of a buffer's composition (*SI Appendix*, Fig. S10). This effect was probably caused by the strong affinity of ApoE to lipoproteins and the steric hindrance caused by the large size of an antibody compared with the small size of lipoproteins (*SI Appendix*, Fig. S6B), consequently making ApoE hard to analyze without usage of strong detergents, and therefore not suitable for high-throughput methods like ELISA. Subsequently, we decided to analyze ApoE protein levels with SDS/PAGE followed by WB (*SI Appendix*, Fig. S11). We found a significant increase in the ApoE level in CSF from PD patients compared with matched controls in 3 independent cohorts (Table 2 and Fig. 3 *A–F*). Using the recombinant ApoE protein, we estimated that the average concentration of ApoE in Stockholm cohort controls was 8.0 μg/mL, while, in PD patients, the average level was 12.6 μg/mL (*SI Appendix*, Fig. S12), nearly

57% more. In contrast, we found no difference in the plasma level of ApoE between controls and PD patients from Stockholm cohort (Fig. 3 *G* and *H*).

The CSF level of ApoE was negatively correlated only with Levodopa Equivalent Daily Doses score (*SI Appendix*, Table S4). No significant correlations were observed between the ApoE level and disease duration, or rating scores from the unified PD rating scale part 3, the Hoehn &Yahr scale, the nonmotor symptoms scale, Beck's depression inventory (BDI), and Montreal cognitive assessment (*SI Appendix*, Table S4). Similarly, there were no correlations between the plasma ApoE level and patient age or any of the PD rating scores (*SI Appendix*, Tables S4 and S5). There was no correlation between plasma and CSF ApoE levels (*SI Appendix*, Table S6).

To investigate the ApoE biomarker potential for PD diagnosis, we performed a receiver operating characteristic (ROC) curve analysis (36, 37) for data obtained from Stockholm cohort. Our analysis showed that, at the level of 0.8 sensitivity, ~0.6 specificity was achievable (*SI Appendix*, Fig. S13A, solid black line). Interestingly, with the same sensitivity of 0.8, we could obtain around 0.7 specificity when only untreated patients were analyzed (*SI Appendix*, Fig. S13A, dashed black line).

ApoE as a Potential Biomarker for Atypical Parkinsonism. To check whether the ApoE increase is specific for PD, we analyzed the level of ApoE in CSF from patients with MSA or PSP from Umeå and Lund cohorts. The ApoE level in MSA patients, another synucleinopathy, was significantly higher compared with controls, whereas its level in PSP patients, a tauopathy, was not significantly changed (*SI Appendix*, Fig. S14). These results further strengthen the relationship between ApoE and αSN.

Uptake of αSN-Enriched Lipoprotein Vesicles in Dopaminergic Neuronal-like Cells. To investigate whether αSN-enriched lipoprotein vesicles can be a possible mechanism of αSN uptake and spreading, we examined the uptake of HDL and VLDL along with αSN-enriched lipoprotein vesicles in neuronal-like cells. We thus differentiated SH-SY5Y human dopaminergic neuroblastoma cells to a neuronal-like state and incubated them with a fluorescently labeled monomeric αSN, HDL, and VLDL, and with double-labeled complexes of αSN-enriched lipoprotein vesicles. We also checked that the labeled αSN does not undergo aggregation or degradation/fragmentation, using both WB and SEC approaches (*SI Appendix*, Fig. S15). We decided not to use unlabeled recombinant αSN, due to the fact that SH-SY5Y cells, which are of human origin, express endogenous αSN. Performing αSN staining in such conditions will not allow discrimination between endogenous and recombinant αSN. Furthermore, we decided to use cells, recombinant proteins, and lipoproteins of human origin to omit any concerns coming from receptor differences across species. After 4-h incubation, we observed that the monomeric αSN alone, as well as HDL and VLDL, easily entered neuronal cells. Interestingly, we observed the same effect for αSN-enriched HDL and VLDL vesicles (Fig. 4), confirming αSN couptake during lipoprotein internalization as a possible mechanism of αSN uptake and spreading.

Immunohistochemical Detection of ApoE in the Human SNc. To examine the distribution of ApoE in the human SN, we performed immunohistochemistry analysis on postmortem human brain tissue from SNc of PD patients and healthy controls. Similarly to previous reports (38, 39), we detected ApoE in paravascular spaces (*SI Appendix*, Fig. S16 *A* and *B*). Moreover, we observed a strong region-specific ApoE signal mostly in periaqueductal gray, intercollicular nucleus, and, most importantly, SNc (*SI Appendix*, Fig. S17 *A–H*). Interestingly, in controls, most of neuromelanin-positive cells (dopaminergic neurons) in SNc were negative (or exceedingly
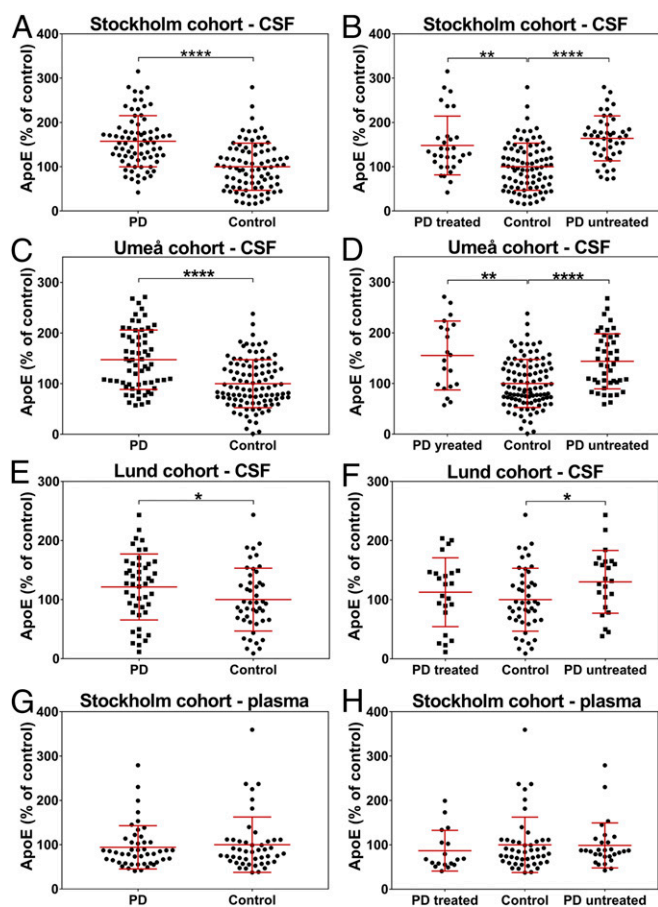

Fig. 3. Levels of ApoE in biofluids from Stockholm, Umeå, and Lund cohorts. (*A*) Stockholm cohort levels of ApoE in CSF of healthy controls compared with PD patients. (*B*) Stockholm cohort levels of ApoE in CSF of healthy controls compared with treated and untreated PD patients. (*C*) Umeå cohort levels of ApoE in CSF of healthy controls compared with PD patients. (*D*) Umeå cohort levels of ApoE in CSF of healthy controls compared with treated and untreated PD patients. (*E*) Lund cohort levels of ApoE in CSF of healthy controls compared with PD patients. (*F*) Lund cohort levels of ApoE in CSF of healthy controls compared with treated and untreated PD patients. (*G*) Stockholm cohort levels of ApoE in plasma of healthy controls compared with PD patients. (*H*) Stockholm cohort levels of ApoE in plasma of healthy controls compared with treated and untreated PD patients. PD, PD. Tests used were the Mann−Whitney *U* test for 2 groups comparison and the Kruskal−Wallis test with the Dunn's correction for more than 2 groups. *P < 0.05; **P < 0.01; ****P < 0.0001.
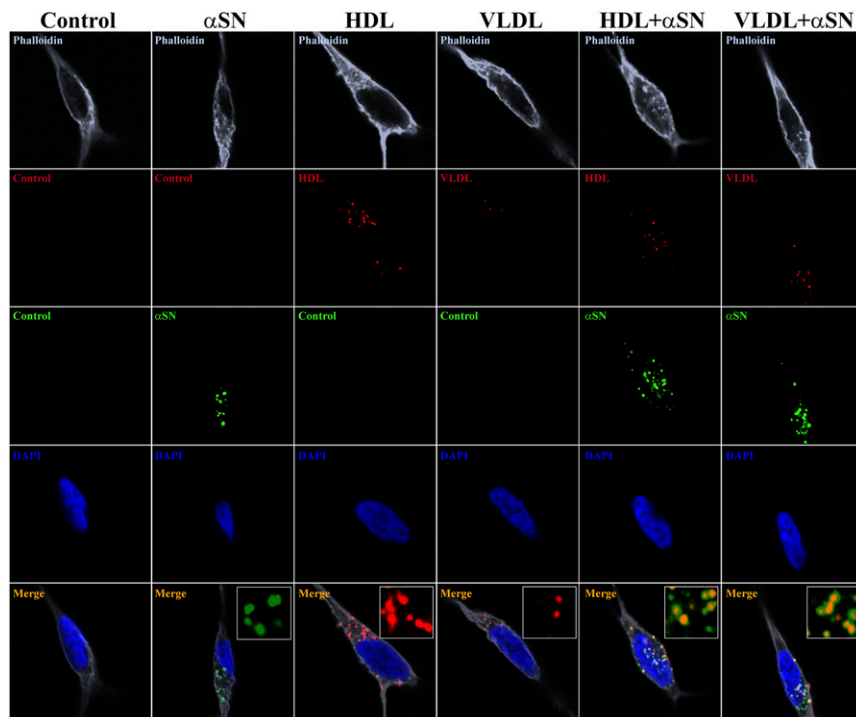
NEUROSCIENCE

Fig. 4. Uptake of lipoprotein vesicles enriched with αSN by SH-SY5Y cells differentiated to dopaminergic neurons. Single-plain confocal images represent the uptake of lipoprotein vesicles enriched with αSN by SH-SY5Y cells differentiated to dopaminergic neurons. (*Left* to *Right*) A vehicle control, uptake of fluorescently labeled αSN-AF488, HDL-AF568, VLDL-AF568, and double-labeled enriched lipoproteins αSN-AF488+HDL-AF568 and αSN-AF488+VLDL-AF568. After 4 d of differentiation, cells were incubated for 4 h with mixtures, then fixed, and proceeded to the F-actin staining with Phalloidin-AF647 and the nuclear labeling with DAPI. *Insets* in merged panels represent magnified areas showing fluorescently labeled αSN and lipoproteins, and their colocalization for enriched vesicles. Images were acquired using 63× magnification objective. *Insets* represent further 5× digital enlargement of 63× magnification images.

low) for the ApoE staining (Fig. 5*A*). In contrast to controls, in sections from PD patients, most of the dopaminergic neurons were clearly positive for ApoE (Fig. 5*A*). Additionally, to confirm observed changes and rule out optical illusion, we performed densitometric analysis of ApoE signal distribution between the intracellular compartment of dopaminergic cells and extracellular space (Fig. 5 *B–D*). We detected a significantly higher signal for extracellular than intracellular ApoE in controls (Fig. 5*B*), while, in PD patients, ApoE signal was distributed equally (Fig. 5*C*). Finally, we compared the ratio of intracellular and extracellular ApoE signal in controls and PD samples and observed a significantly lower ratio for controls, indicating changes in the ApoE gene expression and/or an increased uptake of ApoE in dopaminergic neurons of PD patients. Importantly, we did not observe any ApoE-negative dopaminergic neurons in PD patients, while close cooccurrences of both negative and positive ApoE dopaminergic cells were detected in controls (*SI Appendix*, Fig. S17 *I–K*). Finally, we did not observe any signal on negative control sections in which the primary antibody was omitted (*SI Appendix*, Fig. S16*C*).

Decreased Level of ApoAI in Plasma, but Not in CSF, from PD Patients. We have identified ApoAI as one of the αSN-interacting proteins in CSF (Table 1). The level of ApoAI in CSF was not changed between controls and PD patients (*SI Appendix*, Fig. S18 *A and B* and Table 2). However, in agreement with a previous study (40), we observed a decreased plasma level of ApoAI in PD patients compared with controls (*SI Appendix*, Fig. S18 *C and D* and Table 2). We did not observe any correlation between the level of ApoAI and PD severity scores, disease duration, or age, either in CSF nor in plasma (*SI Appendix*, Tables S4 and S5). However, the CSF level of ApoAI significantly correlated with its IgG and albumin content (*SI Appendix*, Table S5). At the same time, we did not observe any significant changes in albumin and IgG at a group level, either in CSF or in plasma of PD patients and controls (*SI Appendix*, Fig. S19 *A–D*). However, the number of mononuclear cells in CSF was significantly higher in PD pa-

tients compared with controls (*SI Appendix*, Fig. S19 *E and F*), suggesting a mild inflammatory response in PD.

Elevated Levels of ApoJ and ApoCI in CSF, but Not in Plasma, from PD Patients. We also analyzed CSF and plasma levels of 2 other apolipoproteins: ApoJ and ApoCI. The level of ApoJ was significantly increased in CSF (*SI Appendix*, Fig. S20 *A and B* and Table 2), but not in plasma (*SI Appendix*, Fig. S20 *C and D* and Table 2), of PD patients compared with controls. We did not find correlations between the ApoJ level and any PD severity score (*SI Appendix*, Table S4). However, the plasma ApoJ level negatively correlated with age and the albumin content and positively correlated with IgG levels in PD patients (*SI Appendix*, Table S5).

Additionally, we decided to investigate the ApoCI level, due to its high abundance in CSF. Although the level of CSF ApoCI in PD patients did not differ from controls (*SI Appendix*, Fig. S21*A* and Table 2), it was significantly higher in treated compared with untreated PD patients (*SI Appendix*, Fig. S21*B* and Table 2). Furthermore, the ApoCI level in CSF positively correlated with the disease duration, and the plasma level positively correlated with the BDI score (*SI Appendix*, Table S4). We did not observe any difference in the level of ApoCI in plasma between controls and PD patients (*SI Appendix*, Fig. S21 *C and D*). The ApoCI level from controls correlated with albumin and IgG levels in CSF and plasma. For PD patients, ApoC1 levels correlated with albumin and IgG levels in CSF and the albumin level in plasma (*SI Appendix*, Table S5). These data suggest a possible involvement of ApoCI in neuroinflammation rather than a specific contribution to PD.

Correlations between Apolipoproteins Levels in Plasma and CSF and Their Combined Accuracy for PD Detection. As mentioned above, our data strongly indicate differences in levels of various types of apolipoproteins in CSF and plasma of PD patients. Therefore, we investigated whether there is any correlation between levels of different types of apolipoproteins within and between plasma and CSF. We observed that the increased level of ApoE in CSF corresponded to the decreased level of ApoAI in plasma (*SI Appendix*, Table S6). Moreover, we noticed positive correlations
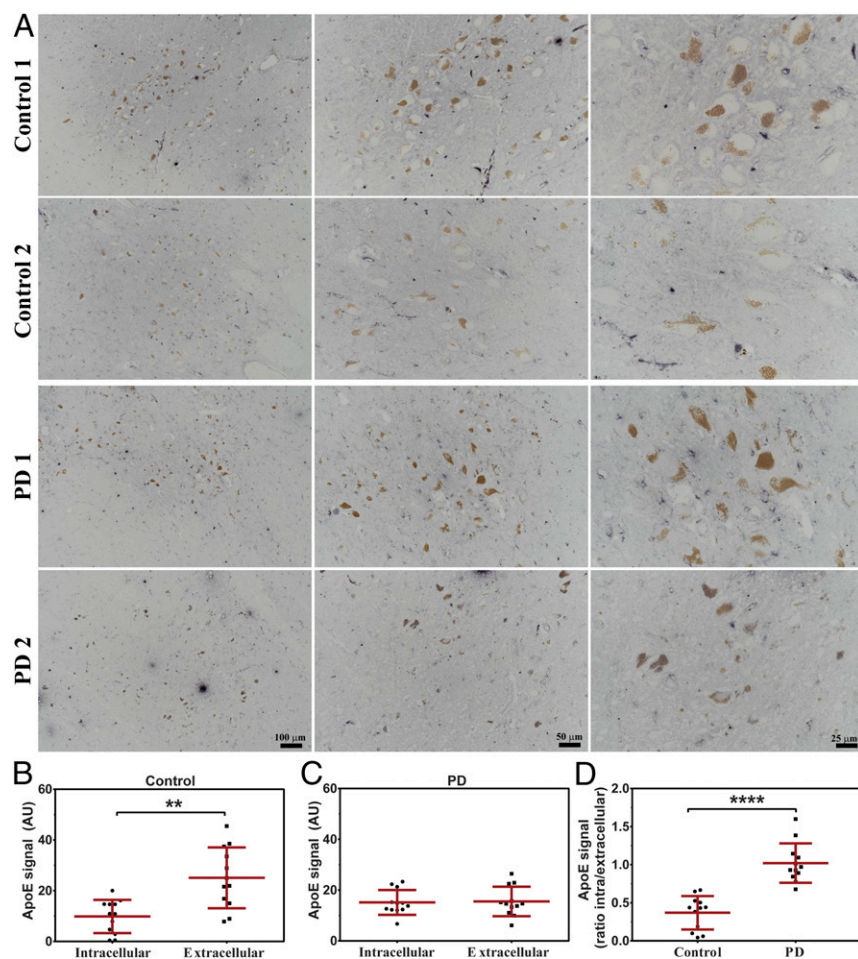
Fig. 5. Analysis of ApoE localization in dopaminergic neurons of the human SN. (*A*) Representative photomicrographs of immunostaining against ApoE in human SN (light blue staining). ApoE immunoreactivity in control individuals (Control 1 and Control 2) present a preferential localization of ApoE to the extracellular space while dopaminergic neurons (brown, neuromelanin-pigmented cells) remain negative (or at very low signal level). Immunostaining against ApoE in brains from PD patients (PD 1 and PD 2) show an equal localization of ApoE in extracellular space and intracellularly in dopaminergic neurons. Scale bars on PD 2 photomicrographs refer to all pictures in the same column. (*B*–*D*) The densitometric analysis of ApoE signal distribution between dopaminergic cells intracellular compartment and extracellular space in (*B*) controls and (*C*) PD patients. (*D*) Ratio of densitometric analysis of intracellular and extracellular ApoE signal between controls and PD patients. Comparison was performed using the Mann–Whitney *U* test. *P* value < 0.05 was considered statistically significant. **$P < 0.01$; ****$P < 0.0001$.

between plasma levels of ApoCI and ApoE as well as between CSF levels of ApoCI and ApoAI. Furthermore, we detected a correlation between plasma levels of ApoJ and ApoAI (*SI Appendix*, Table S6).

In addition, we examined whether a combined ROC analysis of several apolipoproteins would increase the diagnostic accuracy compared with the analysis of ApoE alone. Thus, we combined the level of ApoE in CSF with the level of ApoAI in plasma and recalculated the ROC curve (*SI Appendix*, Fig. S13*B*). We also performed the ROC analysis combining the level of ApoAI in plasma with levels of ApoJ and ApoE in CSF (*SI Appendix*, Fig. S13*C*). Our analysis showed that, with the sensitivity of 0.8, combined levels did not increase the specificity (*SI Appendix*, Fig. S13*D*). However, when the sensitivity was set to 0.71, we could increase the specificity from 0.70 for ApoE alone to 0.83 when combining ApoE, ApoAI, and ApoJ levels (*SI Appendix*, Fig. S13*D*).

Discussion

During the last decade, a number of studies reported that αSN possesses a membrane-binding capacity and can interact not only with artificial lipid vesicles but also with cell membranes and extracellular vesicles, including exosomes (41). Here, using a co-IP approach followed by MS analysis, we discovered a robust interaction between αSN and apolipoproteins in the human CSF. We observed the strongest signal for ApoE, and we further confirmed this interaction using an ELISA method relying on different sets of antibodies. Our data suggest that αSN−apolipoprotein interactions are indirect, since the ApoE protein was not able to interfere with the αSN aggregation, and

we also observed an interaction of αSN with ApoE-negative lipoproteins in vitro. This interaction rather depends on the αSN propensity to bind to the negatively charged lipid particles (42, 43). Importantly, while it is vital to note that both ApoE (44) and αSN (45−47) were found on exosomes, our TEM analysis revealed structures without a clear lipid bilayer. More importantly, we did not identify any exosome markers during the MS analysis, while we observed several apolipoproteins. Our data suggest that αSN associates with lipoprotein particles both in vitro and in human CSF. Approximately 45% of CSF αSN is bound to ApoE-positive lipoproteins. The percentage of αSN bound to ApoE-positive vesicles in CSF is significantly higher in PD patients compared with healthy controls. This is in accordance with the higher level of CSF ApoE in PD patients. It is therefore a rather common event and could be a major mechanism of αSN uptake. At the same time, combining the facts that αSN concentration in CSF is estimated to be around 1 to 2 ng/mL and ApoE concentration is in the range of 5 to 15 μg/mL, we can conclude that this is a rare event from the perspective of lipoproteins. Furthermore, it is likely the amount of αSN−lipoproteins particles taken up by cells will be determined by cellular requirements for lipoprotein cargo. Therefore, αSN−lipoproteins particle uptake will differ between the nonmitotic cell line and fully mature dopaminergic neurons. Moreover, we determined that not only αSN monomers but also oligomers and fibrils can interact with human plasma-derived HDL and VLDL vesicles in vitro. Likewise, during the preparation of this manuscript, it was reported that αSN can interact with lipoproteins also in human plasma (48), further confirming our observations. Finally, we are showing that not only HDL and VLDL alone, but
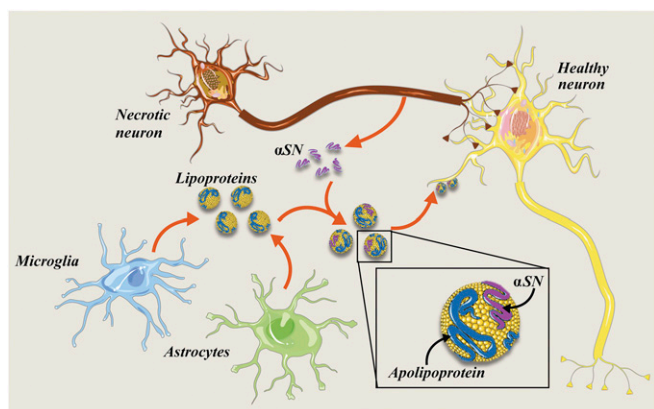
NEUROSCIENCE

Fig. 6. Schematic representing the ApoE and αSN interaction in the human CNS and a possible spreading of a pathological αSN between cells. The pathological and the normal αSN forms might be released form healthy and/or dying neurons to the extracellular space, where they start interacting with lipoprotein particles released by microglia and astrocytes. Further, probably after recognition by lipoprotein receptors, they are taken up by healthy neurons. Possibly, pathological αSN aggregates, resistant to proteolytic cleavage, remain in the cell undigested and become the seed elongated by the normal αSN, which further might lead to neurodegeneration and disease spreading. Image prepared using Smart Server Medical Art (https://smart.servier.com/), which is licensed under CC BY 3.0.

also αSN-enriched lipoprotein vesicles, undergo a cellular uptake by dopaminergic neuronal like cells in vitro. Additionally, we observed compartmentalization of αSN after cellular uptake. This is likely due to the fact that the uptake of lipoproteins, similar to other endocytosis mechanisms, results in trafficking of lipoproteins to endosomes and then to lysosomes (49, 50). Consequently, enrichment of staining in specific cellular compartments is expected.

Taken together, we believe that our present data on αSN–lipoprotein interactions, and their cellular uptake, raise a plausible explanation for the αSN uptake and spreading in the brain. It is possible that the monomeric αSN, as well as hydrophobic aggregates, binds to extracellular lipoprotein particles, which are then taken up by other cells through a lipoproteins endocytosis pathway (Fig. 6). This lipoprotein-dependent mechanism may cooperate with others, including exosome-based and nanotube models, to propagate αSN pathology.

Apolipoproteins themselves are key components of lipoprotein particles and are responsible for the lipid homeostasis as they transport lipids and lipid-soluble compounds from one cell to another (51). The major apolipoprotein in CSF is ApoE, followed by ApoAI, ApoAII, ApoCs, ApoJ, and ApoD (52). The ApoE concentration in the brain is the second highest, following that of liver. In the CNS, ApoE is synthesized mainly by astrocytes and microglia, and, to a certain extent, by immature neurons (53). The ApoE content is high in the paravascular (glymphatic) space, a CSF flow pathway through the brain (39, 54, 55). Moreover, its presence and colocalization with amyloidß in perivascular drainage channels was linked to the ApoE-dependent amyloidß clearance through the blood–brain barrier (56–58).

ApoE levels are increased in injured or stressed neurons and therefore postulated to play a role in the growth and repair of cells in the CNS (59). Furthermore, ApoE allelic variants are linked to an increased risk and earlier age of onset for Alzheimer's disease (34) and cognitive decline in PD (35). While the influence of ApoE genotypes was widely studied in PD, little work has been performed at the protein level (60, 61). We realized that the use of strong detergents is necessary to isolate

ApoE molecules for a proper quantification. For this reason, we analyzed apolipoproteins levels in CSF and plasma with SDS/PAGE followed by WB. Our analysis demonstrated a significant increase of CSF ApoE in PD patients in 3 separate cohorts. Further, by performing the ROC curve analysis, we conclude that measuring apolipoproteins in CSF and plasma can be clinically meaningful, especially when used in combination with other known biomarkers.

ApoE was found to be enriched in the human SN, mostly localized in extracellular or paravascular spaces rather than in the cytosol of dopaminergic neurons. Furthermore, in preliminary studies, we distinguished 2 different populations of neuromelanin-containing dopaminergic neurons: ApoE-positive and ApoE-negative. In controls, the number of ApoE-negative dopaminergic neurons appears higher than the number of ApoE-positive ones. Conversely, in PD patients, the vast majority of remaining neuromelanin-containing neurons appear to be ApoE-positive. However, further analyses are needed to elucidate whether this effect is due to a higher uptake/expression of lipoproteins and/or ApoE-positive neurons being more resistant to neurodegeneration. Furthermore, the results need to be validated in additional PD populations. Nevertheless, our initial observations suggest a functional involvement of ApoE in PD pathology and/or defense against it.

We also studied other apolipoproteins in CSF as well as in plasma. We did not observe any changes in the CSF ApoAI level from PD patients, but, consistent with previous studies, the plasma ApoAI level was decreased (40). Contrary to ApoE, ApoAI in the brain is believed to be plasma-derived (52), while a small amount is synthesized by endothelial cells in the cerebral vasculature (62). This, together with the identified ApoAI−αSN interaction, suggests that toxic αSN species might be transported with ApoAI lipoprotein particles from the periphery and then distributed throughout the brain.

Similar to ApoE, we observed a significant increase in ApoJ levels in CSF from PD patients. Similar to other apolipoproteins, ApoJ, also known as clusterin, is involved in a lipid transportation, but it also serves a chaperone role during the cellular stress response (63). Besides, it stabilizes a range of misfolded proteins (64). Interestingly, ApoJ is involved in the amyloidß clearance through blood–brain barrier (55, 65), and the level of brain ApoJ increases in numerous neurological disorders such as Alzheimer's disease, MSA, ischemia, and epilepsy (66).

Finally, we observed a change in the CSF ApoCI level, but only in treated PD patients. Moreover, CSF and plasma ApoCI levels positively correlated with albumin and IgGs levels, indicating an association of ApoCI with blood−brain barrier integrity and a mild ongoing inflammation.

In summary, the presence of αSN on lipoprotein vesicles in the human CSF, along with the presence of ApoE in some dopaminergic neurons and the cellular uptake of αSN-enriched lipoproteins, represents a possible mechanism for αSN uptake and spreading in the brain. Finally, changes in apolipoproteins' levels in human CSF represent an aspect of PD pathology and can be become clinically meaningful, especially when used in combination with other biomarkers.

1. R. B. Postuma *et al.*, MDS clinical diagnostic criteria for Parkinson's disease. *Mov. Disord.* **30**, 1591–1601 (2015).
2. K. R. Chaudhuri, A. H. V. Schapira, Non-motor symptoms of Parkinson's disease: Dopaminergic pathophysiology and treatment. *Lancet Neurol.* **8**, 464–474 (2009).
3. P. L. McGeer, S. Itagaki, H. Akiyama, E. G. McGeer, Rate of cell death in parkinsonism indicates active neuropathological process. *Ann. Neurol.* **24**, 574–576 (1988).
4. W. G. Meissner *et al.*, Priorities in Parkinson's disease research. *Nat. Rev. Drug Discov.* **10**, 377–393 (2011).
5. M. G. Spillantini *et al.*, Alpha-synuclein in Lewy bodies. *Nature* **388**, 839–840 (1997).
6. S. Chandra, G. Gallardo, R. Fernández-Chacón, O. M. Schlüter, T. C. Südhof, Alpha-synuclein cooperates with CSPalpha in preventing neurodegeneration. *Cell* **123**, 383–396 (2005).
7. J. Lautenschläger, C. F. Kaminski, G. S. Kaminski Schierle, α-Synuclein–regulator of exocytosis, endocytosis, or both? *Trends Cell Biol.* **27**, 468–479 (2017).
8. T. Takenouchi *et al.*, Reduced neuritic outgrowth and cell adhesion in neuronal cells transfected with human alpha-synuclein. *Mol. Cell. Neurosci.* **17**, 141–150 (2001).
9. P. H. Weinreb, W. Zhen, A. W. Poon, K. A. Conway, P. T. Lansbury, NACP, a protein implicated in Alzheimer's disease and learning, is natively unfolded. *Biochemistry* **35**, 13709–13715 (1996).
10. L. Giehm, D. I. Svergun, D. E. Otzen, B. Vestergaard, Low-resolution structure of a vesicle disrupting α-synuclein oligomer that accumulates during fibrillation. *Proc. Natl. Acad. Sci. U.S.A.* **108**, 3246–3251 (2011).
11. W. Paslawski, S. Mysling, K. Thomsen, T. J. Jørgensen, D. E. Otzen, Co-existence of two different α-synuclein oligomers with different core structures determined by hydrogen/deuterium exchange mass spectrometry. *Angew. Chem. Int. Ed. Engl.* **53**, 7560–7563 (2014).
12. M. J. Volles *et al.*, Vesicle permeabilization by protofibrillar alpha-synuclein: Implications for the pathogenesis and treatment of Parkinson's disease. *Biochemistry* **40**, 7812–7819 (2001).
13. J.-Y. Li *et al.*, Lewy bodies in grafted neurons in subjects with Parkinson's disease suggest host-to-graft disease propagation. *Nat. Med.* **14**, 501–503 (2008).
14. F. N. Emamzadeh, Alpha-synuclein structure, functions, and interactions. *J. Res. Med. Sci.* **21**, 29 (2016).
15. C. Betzer *et al.*, Identification of synaptosomal proteins binding to monomeric and oligomeric α-synuclein. *PLoS One* **10**, e0116473 (2015).
16. Y. Zhou *et al.*, Analysis of alpha-synuclein-associated proteins by quantitative proteomics. *J. Biol. Chem.* **279**, 39155–39164 (2004).
17. J. E. Payton, R. J. Perrin, D. F. Clayton, J. M. George, Protein-protein interactions of alpha-synuclein in brain homogenates and transfected cells. *Brain Res. Mol. Brain Res.* **95**, 138–145 (2001).
18. A. Lleó *et al.*, Cerebrospinal fluid biomarkers in trials for Alzheimer and Parkinson diseases. *Nat. Rev. Neurol.* **11**, 41–55 (2015).
19. N. K. Magdalinou *et al.*, A panel of nine cerebrospinal fluid biomarkers may identify patients with atypical parkinsonian syndromes. *J. Neurol. Neurosurg. Psychiatry* **86**, 1240–1247 (2015).
20. B. Mollenhauer *et al.*, Investigating Synuclein Consortium of the Michael J. Fox Foundation for Parkinson's Research, A user's guide for α-synuclein biomarker studies in biological fluids: Perianalytical considerations. *Mov. Disord.* **32**, 1117–1130 (2017).
21. L. Gao *et al.*, Cerebrospinal fluid alpha-synuclein as a biomarker for Parkinson's disease diagnosis: A systematic review and meta-analysis. *Int. J. Neurosci.* **125**, 645–654 (2015).
22. I. Björkhem *et al.*, Oxysterols and Parkinson's disease: Evidence that levels of 24S-hydroxycholesterol in cerebrospinal fluid correlates with the duration of the disease. *Neurosci. Lett.* **555**, 102–105 (2013).
23. S. Hall *et al.*, Cerebrospinal fluid concentrations of inflammatory markers in Parkinson's disease and atypical parkinsonian disorders. *Sci. Rep.* **8**, 13276 (2018).
24. M. Trupp *et al.*, Metabolite and peptide levels in plasma and CSF differentiating healthy controls from patients with newly diagnosed Parkinson's disease. *J. Parkinsons Dis.* **4**, 549–560 (2014).
25. X. Geng *et al.*, α-Synuclein binds the K(ATP) channel at insulin-secretory granules and inhibits insulin secretion. *Am. J. Physiol. Endocrinol. Metab.* **300**, E276–E286 (2011).
26. P. S. Guerreiro *et al.*, LRRK2 interactions with α-synuclein in Parkinson's disease brains and in cell models. *J. Mol. Med. (Berl.)* **91**, 513–522 (2013).
27. K. L. Norris *et al.*, Convergence of parkin, PINK1, and α-synuclein on stress-induced mitochondrial morphological remodeling. *J. Biol. Chem.* **290**, 13862–13874 (2015).
28. W. Paslawski *et al.*, High stability and cooperative unfolding of α-synuclein oligomers. *Biochemistry* **53**, 6252–6263 (2014).
29. M. D. Abramoff, P. J. Magelhaes, S. J. Ram, Image processing with ImageJ. *Biophoton. Int.* **11**, 36–42 (2004).
30. T. G. Redgrave, D. C. K. Roberts, C. E. West, Separation of plasma lipoproteins by density-gradient ultracentrifugation. *Anal. Biochem.* **65**, 42–49 (1975).
31. R. W. Mahley, Central nervous system lipoproteins: ApoE and regulation of cholesterol metabolism. *Arterioscler. Thromb. Vasc. Biol.* **36**, 1305–1315 (2016).
32. W. H. Munroe, M. L. Phillips, V. N. Schumaker, Excessive centrifugal fields damage high density lipoprotein. *J. Lipid Res.* **56**, 1172–1181 (2015).
33. M. C. Chartier-Harlin *et al.*, Apolipoprotein E, epsilon 4 allele as a major risk factor for sporadic early and late-onset forms of Alzheimer's disease: Analysis of the 19q13.2 chromosomal region. *Hum. Mol. Genet.* **3**, 569–574 (1994).
34. C.-C. Liu, C. C. Liu, T. Kanekiyo, H. Xu, G. Bu, Apolipoprotein E and Alzheimer disease: Risk, mechanisms and therapy. *Nat. Rev. Neurol.* **9**, 106–118 (2013). Correction in: *Nat. Rev. Neurol.*, **9**, 184 (2013).
35. K. C. Paul *et al.*, APOE, MAPT, and COMT and Parkinson's disease susceptibility and cognitive symptom progression. *J. Parkinsons Dis.* **6**, 349–359 (2016).
36. C. M. Florkowski, Sensitivity, specificity, receiver-operating characteristic (ROC) curves and likelihood ratios: Communicating the performance of diagnostic tests. *Clin. Biochem. Rev.* **29** (suppl. 1), S83–S87 (2008).
37. K. Hajian-Tilaki, Receiver operating characteristic (ROC) curve analysis for medical diagnostic test evaluation. *Caspian J. Intern. Med.* **4**, 627–635 (2013).
38. P. T. Xu *et al.*, Specific regional transcription of apolipoprotein E in human brain neurons. *Am. J. Pathol.* **154**, 601–611 (1999).
39. T. M. Achariyar *et al.*, Glymphatic distribution of CSF-derived apoE into brain is isoform specific and suppressed during sleep deprivation. *Mol. Neurodegener.* **11**, 74 (2016).
40. C. R. Swanson *et al.*, Lower plasma apolipoprotein A1 levels are found in Parkinson's disease and associate with apolipoprotein A1 genotype. *Mov. Disord.* **30**, 805–812 (2015).
41. C. M. Pfefferkorn, Z. Jiang, J. C. Lee, Biophysics of α-synuclein membrane interactions. *Biochim. Biophys. Acta* **1818**, 162–171 (2012).
42. D. Eliezer, E. Kutluay, R. Bussell , Jr, G. Browne, Conformational properties of alpha-synuclein in its free and lipid-associated states. *J. Mol. Biol.* **307**, 1061–1073 (2001).
43. W. S. Davidson, A. Jonas, D. F. Clayton, J. M. George, Stabilization of alpha-synuclein secondary structure upon binding to synthetic membranes. *J. Biol. Chem.* **273**, 9443–9449 (1998).
44. E. Nikitidou *et al.*, Increased release of apolipoprotein E in extracellular vesicles following amyloid-β protofibril exposure of neuroglial co-cultures. *J. Alzheimers Dis.* **60**, 305–321 (2017).
45. L. Alvarez-Erviti *et al.*, Lysosomal dysfunction increases exosome-mediated alpha-synuclein release and transmission. *Neurobiol. Dis.* **42**, 360–367 (2011).
46. J. Ngolab *et al.*, Brain-derived exosomes from dementia with Lewy bodies propagate α-synuclein pathology. *Acta Neuropathol. Commun.* **5**, 46 (2017).
47. K. M. Danzer *et al.*, Exosomal cell-to-cell transmission of alpha synuclein oligomers. *Mol. Neurodegener.* **7**, 42 (2012).
48. F. N. Emamzadeh, D. Allsop, Alpha-synuclein interacts with lipoproteins in plasma. *J. Mol. Neurosci.* **63**, 165–172 (2017).
49. P. Zanoni, S. Velagapudi, M. Yalcinkaya, L. Rohrer, A. von Eckardstein, Endocytosis of lipoproteins. *Atherosclerosis* **275**, 273–295 (2018).
50. M. M. Al Gadban *et al.*, Differential trafficking of oxidized LDL and oxidized LDL immune complexes in macrophages: Impact on oxidative stress. *PLoS One* **5**, e12534 (2010).
51. R. W. Mahley, S. C. Rall , Jr, Apolipoprotein E: Far more than a lipid transport protein. *Annu. Rev. Genomics Hum. Genet.* **1**, 507–537 (2000).
52. P. S. Roheim, M. Carey, T. Forte, G. L. Vega, Apolipoproteins in human cerebrospinal fluid. *Proc. Natl. Acad. Sci. U.S.A.* **76**, 4646–4649 (1979).
53. Y. Huang, R. W. Mahley, Apolipoprotein E: Structure and function in lipid metabolism, neurobiology, and Alzheimer's diseases. *Neurobiol. Dis.* **72**, 3–12 (2014).
54. Q. Xu *et al.*, Profile and regulation of apolipoprotein E (ApoE) expression in the CNS in mice with targeting of green fluorescent protein gene to the ApoE locus. *J. Neurosci.* **26**, 4985–4994 (2006).
55. J. M. Tarasoff-Conway *et al.*, Clearance systems in the brain—Implications for Alzheimer disease. *Nat. Rev. Neurol.* **11**, 457–470 (2015).
56. D. R. Thal *et al.*, Occurrence and co-localization of amyloid beta-protein and apolipoprotein E in perivascular drainage channels of wild-type and APP-transgenic mice. *Neurobiol. Aging* **28**, 1221–1230 (2007).
57. H. Rolyan *et al.*, Amyloid-beta protein modulates the perivascular clearance of neuronal apolipoprotein E in mouse models of Alzheimer's disease. *J. Neural Transm. (Vienna)* **118**, 699–712 (2011).
58. A. Elali, S. Rivest, The role of ABCB1 and ABCA1 in beta-amyloid clearance at the neurovascular unit in Alzheimer's disease. *Front. Physiol.* **4**, 45 (2013).
59. K. Horsburgh, D. I. Graham, J. Stewart, J. A. Nicoll, Influence of apolipoprotein E genotype on neuronal damage and apoE immunoreactivity in human hippocampus following global ischemia. *J. Neuropathol. Exp. Neurol.* **58**, 227–234 (1999).
60. T. V. Huynh, A. A. Davis, J. D. Ulrich, D. M. Holtzman, Apolipoprotein E and Alzheimer's disease: The influence of apolipoprotein E on amyloid-beta and other amyloidogenic proteins. *J. Lipid Res.* **58**, 824–836 (2017).
61. V. V. Giau, E. Bagyinszky, S. S. An, S. Y. Kim, Role of apolipoprotein E in neurodegenerative diseases. *Neuropsychiatr. Dis. Treat.* **11**, 1723–1737 (2015).
62. H. Weiler-Güttler *et al.*, Synthesis of apolipoprotein A-1 in pig brain microvascular endothelial cells. *J. Neurochem.* **54**, 444–450 (1990).
63. D. T. Humphreys, J. A. Carver, S. B. Easterbrook-Smith, M. R. Wilson, Clusterin has chaperone-like activity similar to that of small heat shock proteins. *J. Biol. Chem.* **274**, 6875–6881 (1999).
64. M. Freixes *et al.*, Clusterin solubility and aggregation in Creutzfeldt-Jakob disease. *Acta Neuropathol.* **108**, 295–301 (2004).
65. S. M. Hammad, S. Ranganathan, E. Loukinova, W. O. Twal, W. S. Argraves, Interaction of apolipoprotein J-amyloid beta-peptide complex with low density lipoprotein receptor-related protein-2/megalin. A mechanism to prevent pathological accumulation of amyloid beta-peptide. *J. Biol. Chem.* **272**, 18644–18649 (1997).
66. G. M. Pasinetti, S. A. Johnson, T. Oda, I. Rozovsky, C. E. Finch, Clusterin (SGP-2): A multifunctional glycoprotein with regional expression in astrocytes and neurons of the adult rat brain. *J. Comp. Neurol.* **339**, 387–400 (1994).

NEUROSCIENCE